

Artifact Removal from the Radial Bioimpedance Signal using Adaptive Wavelet Packet Transform

Pranali C. Choudhari¹, Dr. M. S. Panse²

¹Research Scholar, Department of Electrical Engineering, V.J.T.I., Mumbai, India

² Professor, Department of Electrical Engineering, V.J.T.I., Mumbai, India

ABSTRACT:

Impedance cardiography has become a synonym for indirect assessment of monitoring the stroke volume, cardiac output and other hemodynamic parameters by monitoring the blood volume changes of the body in terms of changes in the electrical impedance of a body segment. Changes occurring in the impedance of the body due to various physiological processes are captured in terms of the voltage variation. But this method is affected by electrical noise such as power line hum and motion and respiratory artifacts due to movement of the subject while acquiring the bioimpedance signal. This can cause errors in the automatic extraction of the characteristic points for estimation the hemodynamic parameters. This paper presents an adaptive algorithm for baseline wander removal from the bioimpedance waveform, obtained at the radial pulse of the left hand, using the wavelet packet transform. The algorithm computes the energy in scale of the wavelet coefficients. The energies in the successive scales are compared and the branch of wavelet binary tree with the higher energy is selected. The impedance signals have been acquired by using the peripheral pulse analyzer and excellent results are obtained.

KEYWORDS: Artifact, Baseline wander, Bioimpedance, Energy, Impedance cardiography, Radial, Wavelet packet transform

I. INTRODUCTION

Time derivative of the thoracic impedance is known as the impedance cardiogram (ICG) and it is used for estimating the ventricular ejection time (T_{LVET}), the negative peak of ICG ($(-dz/dt)_{max}$), the stroke volume, and some other cardiovascular indices. Respiratory and motion artifacts cause baseline drift in the sensed impedance waveform, particularly during or after exercise, and this drift results in errors in the estimation of the parameters [1], [2]. Ensemble averaging [2], a classical statistical technique for baseline cancellation, can be used to suppress the artifacts, but it also subdues the beat-to-beat variations and tends to blunt the peak in the ICG. The characteristics of the waveform which are less distinct may get blurred or even suppressed, thereby resulting in error in the estimation.

Baseline removal has been addressed in many different ways in literature. In [3], baseline estimation method using cubic spline which is a portion of the Maclaurin series (higher than the 4th derivatives are neglected) is proposed. This is a third order approximation where the baseline is estimated by polynomial approximations and then subtracted from the original raw ECG signal. This is a nonlinear method, and its performance is based on estimation of reference points in the PR intervals. The main disadvantage of this method is estimating reference points that may not belong to baseline. In [4], a linear time-varying filtering approach is undertaken to suppress the baseline drift in the ECG signal. Beat average is subtracted from the signal and then decimated. Low-pass filtering is applied to estimate the baseline wander and is interpolated. Then it is subtracted from the original signal. This is a nonlinear approach so it is complex and highly dependent to beat rate calculations and becomes less accurate in low heart rates. Linear filtering is another method applied to baseline wander problem. Using this approach a digital narrow-band linear-phase filter with cut-off frequency of 0.8 Hz has been suggested in [5]. Another filtering technique using digital and hybrid linear-phase with cut-off frequency of 0.64 Hz is used in [6]. Though the method looks quite simple to implement, the number of coefficients used the FIR structure is too high and results in long impulse responses. Most of the baseline wander removal algorithms in the literature have been implemented for denoising the ECG signal and very less work has been done in bioimpedance signals. In addition, there is an overlap on the spectrums of the baseline and

bioimpedance signals. Thus removing baseline spectrum will cause distortion in the signal components also. Time-varying filtering was proposed in [4]. Filter banks with different cut-off frequencies which depend on heart rate and baseline level was implemented. Due to a partial overlap between the spectra of ICG and the artifacts, non-adaptive digital filters are not effective in removing the artifacts. Adaptive filtering may be used for canceling the respiratory artifacts [7], but it is generally difficult to identify the filter parameters related to the sources of various motion artifacts.

II. BIOIMPEDANCE SIGNAL AND THE NOISE ASSOCIATED WITH IT

Bioimpedance is a branch of biophysics concerned with the electrical hindrance offered by biological tissues to the flow of low amplitude, high frequency alternating current (AC). The bioimpedance signal is obtained by applying a constant amplitude AC current across a defined body segment, and the variation in the voltage across this segment is measured. Applying the Ohm's law, this variation in the voltage is directly proportional to the variation in the impedance, as the current is maintained constant. A typical ICG waveform measured across the thorax of the human body and its characteristic points is shown in Fig. 1. Points B, C and X are the three main characteristic of ICG trace. Point B represents opening of the aortic valve, while point X denotes closing of the aortic valve. The point C corresponds to peak of the ICG waveform, while the point X is the lowest point in the ICG waveform. The time interval between point B and point X is the Left Ventricle Ejection Time (LVET) [8]. SV is generally calculated using Kubicek's equation using two hemodynamic parameters: the LVET and the dz/dt_{\max} of ICG [9].

There are two major artifacts in the ICG signal: respiratory and motion artifacts. Respiratory artifacts have very low frequency (0.04-2 Hz), and the frequency of motion artifacts is about 0.1-10 Hz. The baseline drift is due to the respiratory artifacts, while the peaks variation is due to motion artifacts. ICG signal range is 0.8 to 20 Hz, therefore respiratory and motion artifacts lie within the same band [10]. The electrical impedance change caused by blood volume change in aorta typically accounts for 2-4% of the base impedance (usually about 20ohm), while the electrical impedance change caused by the respiratory artifact and motion artifact may be 30% or even more [9]. Therefore the motion and respiratory artifacts may lead to a large baseline drift in the ICG signal, subsequently resulting in errors in characteristic points extraction and calculation of the hemodynamic parameters. ICG signal is modulated by breath which can cause its fluctuation around base impedance Z_0 , thus baseline drift is inevitable during exercise. Subsequently baseline drift might cause inaccurate calculations of hemodynamic parameters when the zero level is used to calculate dz/dt_{\max} . Therefore removing respiratory artifact from ICG signal is prime importance. Moreover, the noise sources such as power line hum, change in impedance of the electrodes due to perspiration can also cause the baseline drift.

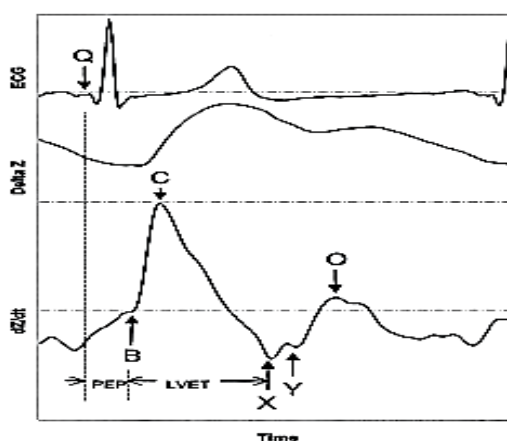


Figure 1: ICG and ECG signals

Wavelets and wavelet packet approximation : There is fair amount overlap in the signal as well as the noise spectra in case of the bioimpedance signal. Hence, the baseline wander elimination algorithm should be able to decompose the signal frequency components into precise levels to clearly distinguish between the signal and the wander. Wavelet decomposition can serve appropriate in this regard. A wavelet system is a set of building blocks from which one can construct or represent a signal or a function. It is a two-dimensional expansion set. The wavelet transform is a time-scale representation method that decomposes signal $x(t)$ into basis functions of time and scale which are dilated and translated versions of a basis function $\psi(t)$ which is called mother wavelet [11,12]. Translation is accomplished by considering all possible integer translations of $\psi(t)$ and dilation is

obtained by multiplying t by a scaling factor which is usually factors of 2. The following equation shows how wavelets are generated from the mother wavelet as given in Eq.1.

$$\psi_{j,k}(t) = 2^{j/2} \psi(2^{j/2}t - k) \tag{1}$$

where j indicates the resolution level and k is the translation in time. This is called dyadic scaling, since the scaling factor is taken to be 2. Wavelet decomposition is a linear expansion and it is expressed as :

$$x(t) = \sum_{k=-\infty}^{\infty} c_k \phi(t - k) + \sum_{k=-\infty}^{\infty} \sum_{j=0}^{\infty} d_{j,k} \psi(2^j t - k) \tag{2}$$

where $\phi(t)$ is called the scaling function or father wavelet and c_k and $d_{j,k}$ are the coarse and detail level expansion coefficients, respectively. Eq. 2 effectively means finding projections of the signal on the basis functions for the approximation and detail branches, $\phi(t)$ and $\psi(t)$ respectively. In practice, one never has to deal with the basis functions. Finding projections on approximation level basis function essentially means averaging or passing the signal through a low pass filter, while the detail level basis function high pass filters the signals as shown in Fig.2.

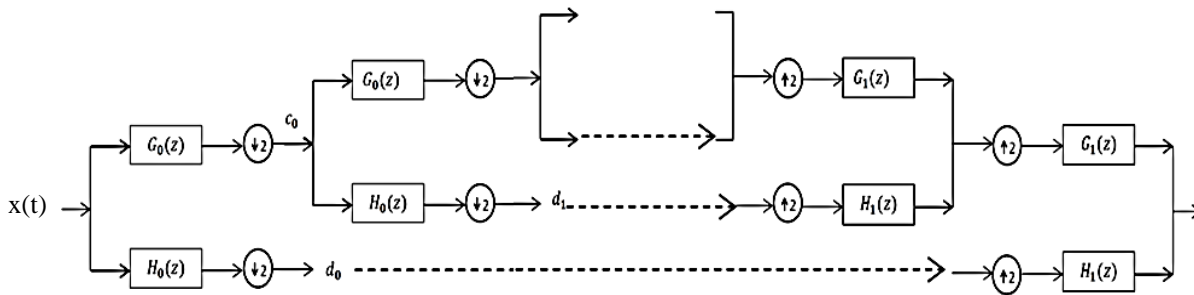


Figure 2: Filter bank representation of wavelet decomposition

Here $G_0(z)$ and $H_0(z)$ are essentially low pass and high pass filters respectively, which split the signal bandwidth into half. To achieve the next level decomposition, the approximation coefficient is further passed through this quadrature mirror filter bank formed by the low and high pass filters. These filters are related to wavelet $\psi(t)$ and scaling functions $\phi(t)$ as expressed below [13]:

$$\psi(t) = \sum_k \sqrt{2} h_0(k) \phi(2t - k) \tag{3}$$

$$\phi(t) = \sum_k \sqrt{2} g_0(k) \phi(2t - k) \tag{4}$$

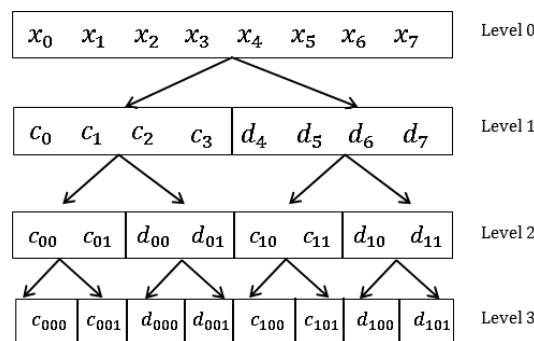


Figure 3: Wavelet Packet decomposition tree

Wavelets are useful in applications such as signal denoising, wave detection, data compression, feature extraction, and so forth. There are many techniques based on wavelet theory, such as wavelet packets, wavelet approximation and decomposition, discrete and continuous wavelet transform etc. The basic wavelet transform has only one-sided decomposition of the approximate coefficients. This is not sufficient in removal of noise sometimes. Hence to obtain more flexibility, the detail coefficient can also be decomposed in approximate and detail branches as shown in Fig.3. This aids in exploring the other frequency bands to correctly estimate the noise signal.

III. PROPOSED ALGORITHM

The algorithm for baseline wander removal using wavelet packet decomposition has been proposed in this paper. The algorithm is based on the assumption that the baseline drift signal is mixed with the bioimpedance signal in a linear fashion. The signal is not obtained using the usual thoracic impedance cardiography technique. It is rather obtained on the radial pulse (wrist of the left hand). The volume of blood flow in this section of the body is much smaller as compared to the thoracic region, due to the smaller diameters of the blood carrying vessels in this region as compared to the aorta. Hence the amount of variation in the impedance due to the pulsatile blood flow is also much smaller. In addition to the spectral overlap between the signal and drift, the amplitudes of the two signals are also comparable; thus making the process of drift removal even more challenging. Fig.4 shows the flowchart for estimation and cancellation of the baseline wander. First, the wavelet packet decomposition of the bioimpedance signal is computed.

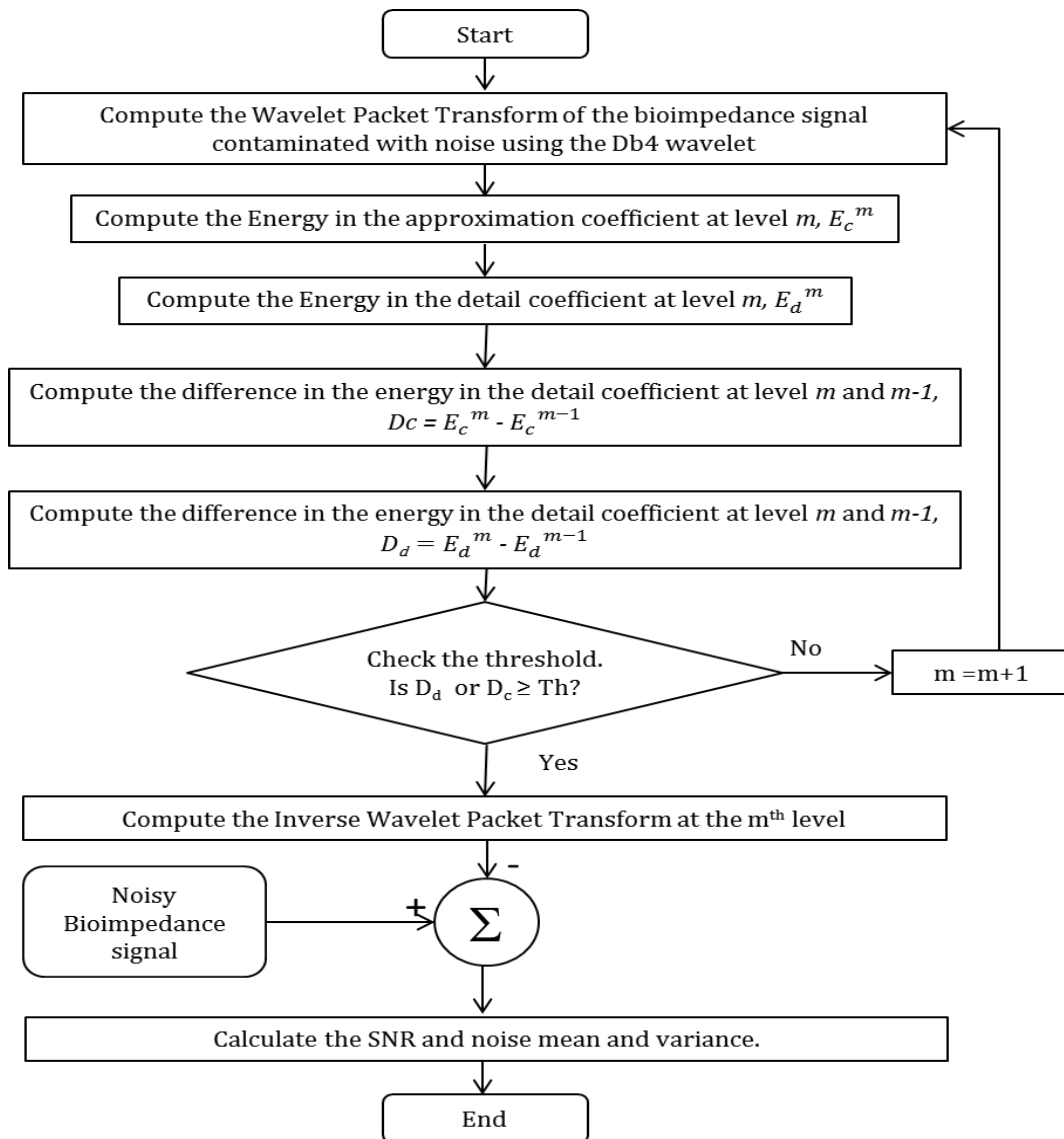


Figure 4: Flowchart of bioimpedance baseline drift removal algorithm

Since the high frequency components are highlighted at low level scales, it is expected to observe the baseline drift at larger scales. The energy of a signal is given in terms of the wavelet coefficients by Parseval's relation as

$$\int |f(t)|^2 dt = \sum_{i=0}^{\infty} |c_i|^2 + \sum_{j=0}^{\infty} \sum_{k=-\infty}^{\infty} |d_{jk}|^2 \quad (5)$$

At each step the energy of both, the approximation as well as the detail coefficients is calculated. The branch with the higher energy is decomposed further. This will be followed till the energy difference in the subsequent levels exceeds the preset threshold value. The algorithm adaptively computes the preset threshold for each signal. It was experimentally observed that, whenever this value is between 0.7 % to 2% of the energy of the original signal, the last scale has been reached. Taking an average value of 1.0875% of the signal energy, gave acceptable results for all the subjects.

IV. SIMULATION RESULTS

In this section, the results of the proposed algorithm for different signals are presented to illustrate the effectiveness of the algorithm. The dyadic wavelet packet decomposition of the signal at a given level represents the projections of the signal on the basis functions of that level. To ensure that the representation is most accurate, the basis function should have higher resemblance with the signal variations. Initially the decomposition was carried out using the Daub-4 mother wavelet, Bior 2.8 and Symlet 4, and the one which gave highest SNR was selected. Table 5.1 and Table 5.2 show the noise mean, noise variance and SNR obtained with each of these wavelets. The Daub-4 scaling function resembles the bioimpedance signal the most. The noise, SNR obtained using the Daub-4 is also better than the other two. Thus the wavelet packet decomposition of the signal was done using Daub-4 wavelet. The time of execution and thus the number of levels of decomposition were also found to be lesser in case of Daub-4. Fig. 5 shows the results of the baseline wander removal algorithm for five subjects with wavelet packet decomposition using Daub-4 mother wavelet. Decrease in the variance is calculated as :

$$\% \text{ Decrease in variance} = \frac{\text{var}(\text{noisy signal}) - \text{var}(\text{clean signal})}{\text{var}(\text{noisy signal})} \times 100$$

Table 5.1 Comparison of noise mean, noise variance and reduction in signal variance after noise removal with different wavelet functions

Subject	Noise mean			Noise variance			% Decrease in variance		
	db4	bior 2.8	sym 4	db4	bior 2.8	sym 4	db4	bior 2.8	sym 4
Subject 1	73.746	73.746	73.747	57.901	57.237	57.515	76.571	76.369	76.781
Subject 2	75.437	75.435	75.435	56.956	57.956	56.378	71.051	69.838	70.219
Subject 3	76.001	76.001	76.001	68.465	68.105	68.036	87.610	85.844	85.751
Subject 4	79.098	79.099	79.098	45.246	45.191	44.802	84.829	81.939	81.136
Subject 5	76.879	76.878	76.878	249.822	248.390	246.387	94.457	91.647	94.396

Table 5.1 Comparison of SNR after noise removal and the time required for execution with different wavelet functions

Subject	SNRout (DB)			Time for execution (sec)		
	db4	bior 2.8	sym 4	db4	bior 2.8	sym 4
Subject 1	28.682	24.550	24.612	0.814	0.914	0.874
Subject 2	29.354	25.053	23.289	0.835	0.835	0.872
Subject 3	26.947	26.897	26.974	0.891	0.891	0.868
Subject 4	26.404	26.551	26.603	0.752	0.952	0.835
Subject 5	29.391	26.495	26.622	1.014	1.214	1.067

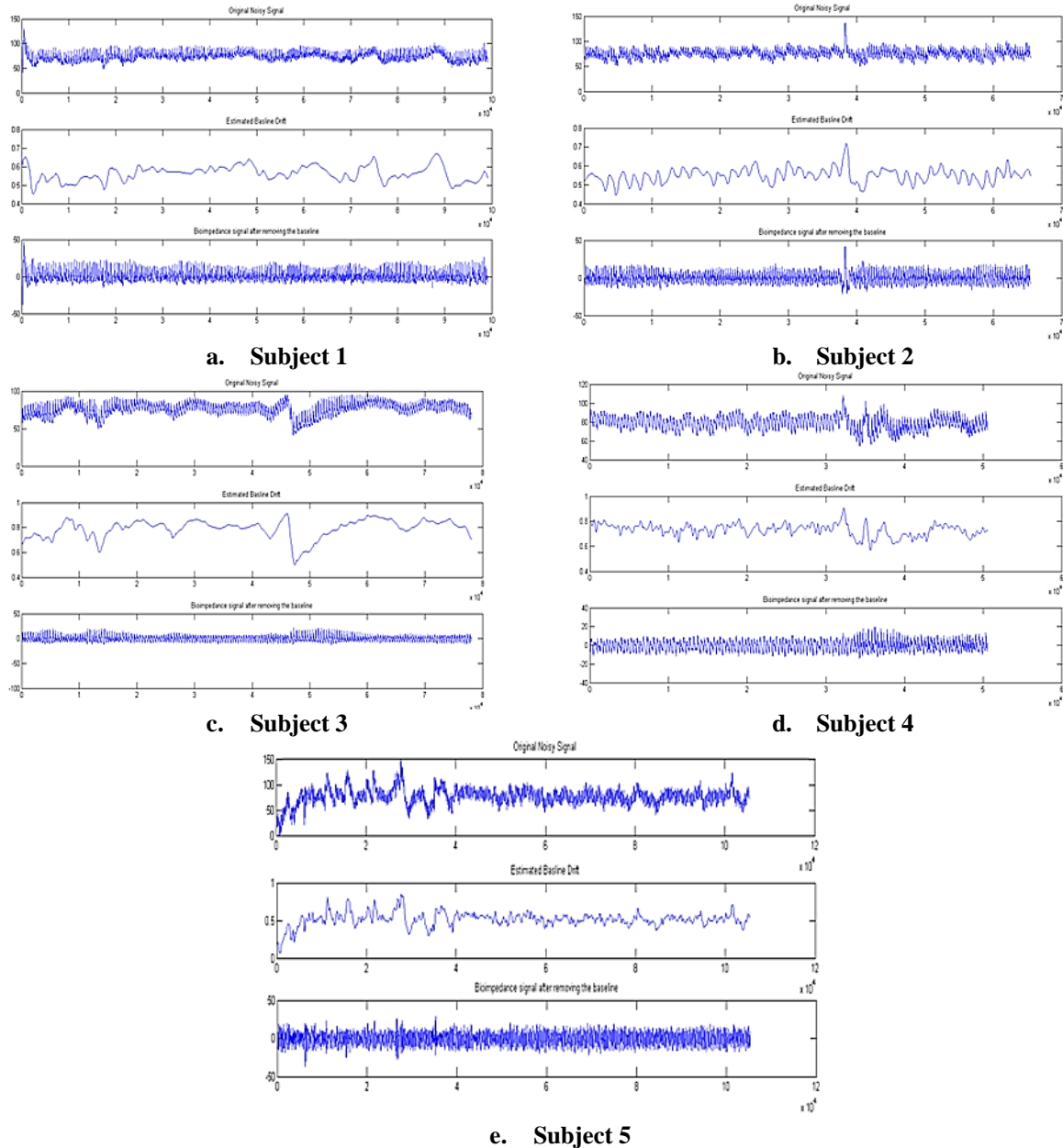


Figure 5: Filtered results obtained with the proposed baseline wander algorithm for five subjects

V. CONCLUSION

The bioimpedance signal is of great importance in calculating the cardiac output, stroke volume and other cardiovascular parameters. It is of utmost importance to correctly locate the characteristic points on the signal, thereby avoiding error estimation of the parameters for diagnosis. Various baseline wander removal algorithms have been implemented in the literature, but the major challenge in this implementation was the spectral overlap between the noise and the signal and comparable amplitudes. Since the signals were acquired at the wrist of the left hand, the original signal itself was weaker in amplitude. It was extremely important to preserve the energy and characteristic points of the signal after removal of the baseline drift. The proposed adaptive wavelet packet based algorithm removes the baseline wander and preserve the clinical information of the bioimpedance records, without introducing any deformities in the signal. Since the number of levels of decomposition are calculated using the energy of the signal itself, each signal receives a different treatment for removal of the baseline drift. Eight to ten levels of dyadic wavelet packet decomposition were needed in each of the subject for correctly estimating the baseline drift.

REFERENCES

- [1] R. P. Patterson, "Fundamental of impedance cardiography," *IEEE Eng. Med. Biol. Mag.*, vol. 8, pp. 35-38, Mar. 1989.
- [2] B. E. Hurwitz et al., "Coherent ensemble averaging techniques for impedance cardiography," in *Proc.3rd Annu. IEEE Symp. Comp. Based Med. Syst.*, June 1988.
- [3] C. R. Meyer and H. N. Keiser, "Electrocardiogram baseline noise estimation and removal using cubic splines and statespace computation techniques," *Computers and Biomedical Research*, vol. 10, no. 5, pp. 459–470, 1977.
- [4] L. Sornmo, "Time-varying filtering for removal of baseline wander in exercise ECGs," in *Proceedings of Computers in Cardiology*, pp. 145–148, Venice, Italy, September 1991.
- [5] J. A. Van Alste and T. S. Schilder, "Removal of base-line wander and power-line interference from the ECG by an efficient FIR filter with a reduced number of taps," *IEEE Transactions on Biomedical Engineering*, vol. 32, no. 12, pp. 1052–1060, 1985.
- [6] I. I. Christov, I. A. Dotsinsky, and I. K. Daskalov, "High-pass filtering of ECG signals using QRS elimination," *Medical and Biological Engineering and Computing*, vol. 30, no. 2, pp. 253– 256, 1992.
- [7] V. K. Pandey and P.C. Pandey, "Cancellation of respiratory artifacts in impedance cardiography," in *Proc. IEEE/ EMBC 2005*. pp. 5503- 5506,2005.
- [8] Marquez JC, Rempfler M, Seoane F and Lindecrantz K. Textrode-enabled transthoracic electrical bioimpedance measurements-towards wearable applications of impedance cardiography. *Journal of Electrical Bioimpedance: Vol. 4*; pp. 45 -50; 2013.
- [9] Vinod KP, Prem CP, Nitin JB, and Subramanyan LR. Adaptive Filtering for Suppression of Respiratory Artifact in Impedance Cardiography. *33rd Annual International Conference of the IEEE EMBS: Boston, Massachusetts USA; August 30-September 3; 2011*.
- [10] Piskulak P, Cybulski G, Niewiadomski W, and Paalko T. Computer Program for Automatic Identification of Artifacts in Impedance Cardiography Signals Recorded during Ambulatory Hemodynamic Monitoring. *XIII Mediterranean Conference on Medical and Biological Engineering and Computing 2013: IFMBE Proceedings 41*, 2013
- [11] Gadre VM. *Wavelets and Multirate Digital Signal Processing. Lecture 42: Application Assignment: Wavelet Based Denoising.*
- [12] S. Mallat, *A Wavelet Tour of Signal Processing*, Academic Press, San Diego, Calif, USA, 2nd edition, 1999.
- [13] I. Daubechies, *Ten Lecture on Wavelets*, SIAM, Philadelphia, Pa, USA, 1992.